

Critical current from dynamical boundary instability for fully frustrated Josephson junction arrays

Beom Jun Kim and Petter Minnhagen

Department of Theoretical Physics, Umeå University, 901 87 Umeå, Sweden

We investigate numerically the critical current of two-dimensional fully frustrated arrays of resistively shunted Josephson junctions at zero temperature. It is shown that a domino-type mechanism is responsible for the existence of a critical current lower than the one predicted from the translationally invariant flux lattice. This domino mechanism is demonstrated for uniform-current injection as well as for various busbar conditions. It is also found that inhomogeneities close to the contacts makes it harder for the domino propagation to start, which increases the critical current towards the value based on the translational invariance. This domino-type vortex motion can be observed in experiments as voltage pulses propagating from the contacts through the array.

PACS numbers: 74.50.+r, 74.60.Ge, 74.60.Jg

The two-dimensional (2D) Josephson junction arrays (JJA's) are ideal testing grounds for static and dynamic properties related to vortices and constitute an intriguing field of physics by itself.¹ They can be fabricated with high precision and are ideally suited for experiments and simulation studies, as well as theoretical approaches.¹ Vortex physics is also of great importance for understanding the properties of high- T_c superconductors, in particular, the interplay between vortex correlations, pinning, and dynamics.² The present paper describes an interesting example of such an interplay. It focuses on what happens at the current threshold for the onset of resistance in the case of a 2D JJA in a perpendicular magnetic field. The threshold is in such a case caused by the onset of motion of the vortices induced by the external magnetic field. We find that this onset of vortex motion is caused by a domino-type effect corresponding to voltage pulses traveling through the sample.

The value of the critical currents in 2D JJA's have been investigated theoretically by several authors.³ These studies have revealed that the zero-temperature critical current I_c depends strongly on the value of the frustration f defined by the number of flux quanta per plaquette induced by the external magnetic field, and they unanimously have obtained the value $I_c = \sqrt{2} - 1 \approx 0.41$ (in units of the critical current of a single junction) for the fully frustrated ($f = 1/2$) square array. On the other hand, numerical calculations based on the resistively shunted junction (RSJ) model with the uniform-current injection method (see Ref. 4 for details) have persistently given the value $I_c = 0.35(1)$.⁴⁻⁸ The discrepancy has usually been attributed to either finite-size effects or an artifact of the uniform-current injection method, but without any really substantiating evidence for either claim. As to the first suggestion, the same numerical value has now been found in a very large array (256×256) (Ref. 8) and the absence of any size dependence up to this array size appears to preclude the possibility of an explanation in terms of finite-size effects. The second possibil-

ity also by now seems less likely since attempts to model the injection of current through busbars, in close analogy with actual experimental situations (see Ref. 9 for details), in fact seem to give an even smaller value.^{5,7,8} Furthermore, in Ref. 7 an improved busbar method was proposed and $I_c \approx 0.35$, close to the one obtained for the uniform-current injection, was found. Thus a value lower than the theoretically predicted one has been obtained with a variety of injection methods.

In the present paper we resolve this long-standing discrepancy and find that the true critical current is in fact lower than the theoretically predicted one and corresponds to a domino-type mechanism starting from the contacts which breaks the translational invariance of the vortex lattice. This means that the theoretically predicted value, which presumes translational invariance, in fact gives an upper limit of I_c . We conclude that the true critical current is always lower and that the precise value, because it is given by a domino mechanism, is sensitive to the inhomogeneities close to the contacts.

We numerically study the fully frustrated $L_x \times L_y$ RSJ square arrays at zero temperature. We use the periodic boundary condition in the y direction and the external current I_d is inserted on the left boundary ($x = 0$) and the extracted on the right boundary ($x = L_x$). The current I_{ij} from site i to site j is the sum of the supercurrent and the normal current:

$$I_{ij} = J_{ij} \sin(\theta_i - \theta_j + A_{ij}) + \dot{\theta}_i - \dot{\theta}_j,$$

where J_{ij} is the critical current of the single junction, the fully frustrated case corresponds to the magnetic bond angle $A_{ij} = \pi x$ for all vertical links at x and zero for all links in the x direction, and finally, $\dot{\theta}_i - \dot{\theta}_j$ is the normal current (in a convenient unit system). The RSJ equations are obtained by demanding current conservation on each site⁴ and are integrated either by starting from the ground-state configuration found from the simulated annealing Monte Carlo method for $I_d = 0$ or from a random configuration. The current injection methods are shown

in Fig. 1 and are as follows: The uniform-current (UC) injection method⁴ corresponds to $J_{ij} = 1$ for all links [Fig. 1(a)]; the conventional busbar (CB) method⁹ where the links on the boundaries have large J_{ij} corresponding to a superconducting busbar (we use $J_{ij} = 10$ for the fat links in Fig. 1); Simkin's improved busbar (SB) method⁷ where in addition to the superconducting busbar there are no magnetic fields on the plaquettes adjacent to the boundaries [Fig. 1(c)]; the busbar method with inhomogeneities near the boundaries (IB) [Figs. 1(d) and (e) are two variants, IB1 and IB2, respectively]. The idea behind these inhomogeneities close to the contacts is that they create barriers for the onset of the vortex motion. The fat horizontal links in Figs. 1(d) and (e) play the role of such barriers.

The translationally invariant ground state is a checkerboard pattern with a vortex at every second plaquette [see Fig. 2(a)]. Let us first assume the translational symmetry even when an external current I_d is turned on. Every second horizontal junction will then by symmetry have the same current and we below focus on the horizontal junctions with the largest current. For some external current $I_d = I_s$ the current through these links reaches the maximum supercurrent for a single junction, which is 1 in our current unit. A straightforward calculation shows that this occurs at $I_s = (3 - \sqrt{5})/2$ (see Table I). For $I_d < I_s$ the ground state vortex configuration is always stable. However, at some $I_d = I_c \geq I_s$ this ground state configuration becomes unstable and dissipation sets in. In the translationally invariant case this happens at $I_c = \sqrt{2} - 1$ (see Table I),¹⁰ which can readily be verified with the boundary condition in Ref. 8 which preserves the translational invariance; $I_c = 0.4142(1)$ has been obtained in excellent agreement with the prediction $\sqrt{2} - 1$.

In reality, however, the current pattern enforced by the contacts is not fully compatible with the translationally invariant vortex pattern. One consequence of this is that the external current I_{sb} needed before a horizontal junction at the boundary reaches its maximum supercurrent is lower than for the translationally invariant case. Table I gives the actual values for the boundary conditions shown in Fig. 1 together with the vortex column for which it occurs. This lower value of I_{sb} suggests that the vortex columns close to the contacts may start to move and dissipate energy before the rest of the vortices. Figure 2 illustrates some of the possibilities: The transition from Fig. 2(a) to 2(b) is the translationally invariant case where the whole vortex lattice moves in one piece. The transition from Fig. 2(a) to 2(c) followed by 2(c) to 2(a) illustrates the case when only the vortex column closest to the boundary moves and the others remain fixed. Note that this is a boundary effect in the sense that it only produces a voltage drop for the horizontal junctions closest to the contacts and no voltage drop across the rest of the sample. Another possibility is that the motion of the first vortex column [Fig. 2(a) to 2(c)] is followed by the second column [as illustrated by

Fig. 2(c) to 2(d)], and then followed by the third and so on without stopping. Such a consecutive motion of vortex columns starting from the contacts and continuing without stopping we refer to as a domino-type motion. We have found that this domino-type motion starts at a lower current than what is required for the translationally invariant motion and that consequently the threshold current for the domino motion is the true critical current. Thus the domino effect is responsible for the critical current for all the boundary conditions shown in Fig. 1 and the corresponding values are given in Table I.

The domino instability has two basic ingredients: The first is that the boundary and current injection break the translationally invariant current pattern close to the boundary which lowers the threshold current for the first vortex column to move. This is related to that I_{s1} for the first column is smaller than I_s for the translationally invariant case (see Table I). The second ingredient is that this motion creates an instability which propagates through the whole sample. A hand-waving argument for this goes as follows: One first notes that as long as the checkerboard pattern of vortices is present a horizontal junction with lower current is always followed by one of higher current. However, when the first column moves [as illustrated by Fig. 2(a) to 2(c)] then two vortices become neighbors. This means that now two horizontal junctions with higher currents follow each other. Because of current conservation this means that the junctions in the second column with higher currents will momentarily further increase which makes this column unstable. The motion of the second column in the same fashion causes the third column to become unstable and so on.

Figures 3(a) and (b) illustrate the domino mechanism for the uniform current injection: Figure 3(a) shows that the voltage is zero up to a critical current I_c . The fact that the voltage per length saturates to a nonzero value above I_c as the distance between the contacts is increased, demonstrates that it is a true onset of dissipation across the whole sample. Figure 3(b) shows the voltage drop $V(x, t)$ at time t for the horizontal junction at position x along a row of junctions in the presence of a current slightly larger than the critical current [$I_d = 0.36 > I_c = 0.350(1)$]. As seen the voltage pulse always travels from one of the contacts towards the opposite in accordance with the domino mechanism. In addition, the interference between domino propagations traveling in opposite directions creates interesting pattern in this 3D plot. A measurable consequence of this is that, if the voltage drop across different positions along the current direction is measured as a function of time, then traveling voltage pulses can be observed. This is in contrast to the translationally invariant case where the voltage appears at the same time along the whole current direction as is illustrated in Fig. 3(c). This translationally invariant case is simulated with the fluctuating-twist-boundary method, as is described in Ref. 8.

The domino mechanism applies to all the situations shown in Fig. 1 with some variants: For example, in the

case of the conventional busbar injection [see Fig. 1(b)] the first vortex column becomes unstable at a current I_{cb} but the domino avalanche does not set in until a larger current I_c is applied (see Table I). This is illustrated in Fig. 4, which shows the onset of dissipation at I_{sb} for a finite system and a further increase at I_c . However, as the distance between the contacts becomes larger dissipation between I_{cb} and I_c decreases towards zero. The situation between I_{cb} and I_c is hence a boundary effect of the type illustrated by Fig. 2(a) to 2(c) followed by 2(c) to 2(a), i.e., only the first column moves.

In Ref. 10 the critical current for a fully frustrated square array of Josephson junctions was measured and found to be $I_c \approx 0.42(2)$.¹¹ As apparent from Table I this value is larger than what is obtained for the RSJ model with uniform-current injection [Fig. 1(a)] and busbar injections [Fig. 1(b) and (c)] and is in fact close to the translationally invariant value. This means that the domino mechanism is somehow suppressed. One way of suppressing this mechanism is to introduce barriers close to the boundary which prevents the domino avalanche from spreading. The situation in Fig. 1(d) shows an extreme variant of this and as seen from Table I this results in a critical current close to the translationally invariant case. However, also in this case the domino mechanism is responsible for the onset of dissipation. Thus the translationally invariant value appears to be an upper limit and the true critical current is always lower and given by the domino mechanism. A perhaps more realistic situation is with some imperfections close to the boundaries which creates barriers for the vortex motion like in Fig. 1(e) and as seen from Table I the critical current is again close to the translationally invariant value. Figure 5 shows the domino mechanism for this case in a 3D plot. [Note the similarity with Fig. 3(b).]

The time scale of the Josephson junction array is given by $t_0 = \hbar/2eR_N J$ with the shunt resistance R_N . For the 1000×1000 SNS junction array in Ref. 10 where $R_N \approx 2$ m Ω and $J \approx 7$ mA this means $t_0 \approx 10^{-11}$ sec. The time for a voltage pulse to reach the middle would then for the uniform current injection [Fig. 3(b)] as well as for the case with inhomogeneities (Fig. 5) be of the order of 10^{-7} sec. Thus it seems that it should be possible to verify the domino mechanism by either direct voltage measurements or by some vortex imaging technique.¹²

In summary, on the basis of simulations for the RSJ model, we have concluded that the critical current for a 2D fully frustrated Josephson junction array is due to a domino mechanism and that the voltage pulses resulting from the domino avalanches should be open to experimental verification.

Discussions with C. J. Lobb, R. S. Newrock, and S. Teitel are gratefully acknowledged. The research was supported by the Swedish Natural Science Research Council through Contract No. FU 04040-322.

- ¹ For a recent review on JJA's see, e.g., R.S. Newrock, C.J. Lobb, U. Geigenmüller, and M. Octavio, Solid State Physics, edited by H. Ehrenreich and S. Spaepen (Academic Press, New York, in press).
- ² G. Blatter, M.V. Feigel'man, V.B. Geshkenbein, A.I. Larkin, and V.M. Vinokur, Rev. Mod. Phys. **66**, 1125 (1994),
- ³ S. Teitel and C. Jayaprakash, Phys. Rev. Lett. **51**, 1999 (1983); W.Y. Shih and D. Stroud, Phys. Rev. B **32**, 158 (1985); T.C. Halsey, *ibid.* **31**, 5728 (1985).
- ⁴ K.H. Lee, D. Stroud, and J.S. Chung, Phys. Rev. Lett. **64**, 962 (1990); K.H. Lee and D. Stroud, Phys. Rev. B **43**, 5280 (1991).
- ⁵ J.U. Free, S.P. Benz, M.S. Rzchowski, M. Tinkham, C.J. Lobb, and M. Octavio, Phys. Rev. B **41**, 7267 (1990).
- ⁶ M. Octavio, J.U. Free, S.P. Benz, R.S. Newrock, D.B. Mast, and C.J. Lobb, Phys. Rev. B **44**, 4601 (1991).
- ⁷ M.V. Simkin, Phys. Rev. B **57**, 7899 (1998).
- ⁸ B.J. Kim and P. Minnhagen, Phys. Rev. B **60**, 588 (1999).
- ⁹ M.V. Simkin and J.M. Kosterlitz, Phys. Rev. B **55**, 11646 (1997).
- ¹⁰ S.P. Benz, M.S. Rzchowski, M. Tinkham, and C.J. Lobb, Phys. Rev. B **42**, 6165 (1990).
- ¹¹ This is estimated from the maximum of dV/dI which occurs at a slightly higher value than the true threshold.
- ¹² S.G. Lachenmann, T. Doderer, R.P. Huebener, T.J. Hagenaars, J.E. van Himbergen, P.H.E. Tiesinga, and J. V. José, Phys. Rev. B **56**, 5564 (1997); P. Binder, D. Abaimov, A.V. Ustinov, S. Flach, and Y. Zolotaryuk, Phys. Rev. Lett. **84**, 745 (2000); A. Tonomura, H. Kasai, O. Kamimura, T. Matsuda, K. Harada, J. Shimoyama, K. Kishio, and K. Kitazawa, Nature (London) **397**, 308 (1999).

TABLE I. The critical current (I_c), the boundary critical current for the motion of the first vortex column (I_{cb}), and the external current needed for the first junction to reach its maximum current (I_{sb}) (in I_{si} , $i=1,2,5$ denotes the column it occurs in). TI denotes the translationally invariant case; see Fig. 1 for the other current injection methods.

	I_c	I_{cb}	I_{sb}
TI	$\sqrt{2} - 1 \approx 0.4142$		$I_{sb} = I_s = (3 - \sqrt{5})/2 \approx 0.382$
UC	0.350(1)		$I_{s1} = 0.285(1)$
CB	0.324(1)	0.277(1)	$I_{s1} = 0.183(1)$
SB	0.337(1)		$I_{s2} = 0.265(1)$
IB1	0.4135(5)		$I_{s5} = 0.366(1)$
IB2	0.4138(5)	0.281(1)	$I_{s1} = 0.249(1)$

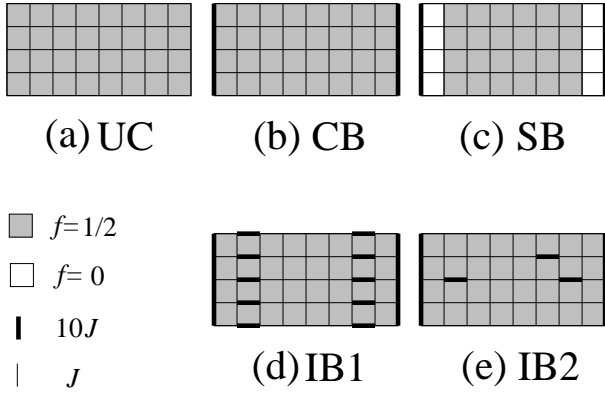


FIG. 1. Current injection methods: (a) Uniform current (UC) injection method, (b) conventional busbar (CB), (c) busbar method in Ref. 7 where unfrustrated columns ($f=0$) are used near busbars (SB). (d) and (e) show busbar methods with inhomogeneities near boundaries (IB1 and IB2, respectively). The fat links have a much larger coupling strength than the normal links.

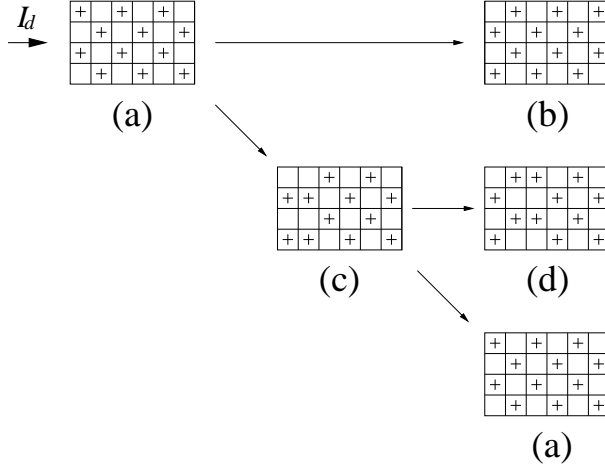


FIG. 2. The configuration with translational symmetry in (a) can evolve in different ways: From (a) to (b), the translational symmetry is preserved by the rigid motion of vortices. From (a) to (c), only one column near boundary moves. Once the motion (a) to (c) happens, this unstable vortex configuration can be resolved by the motion either to (d) or to (a).

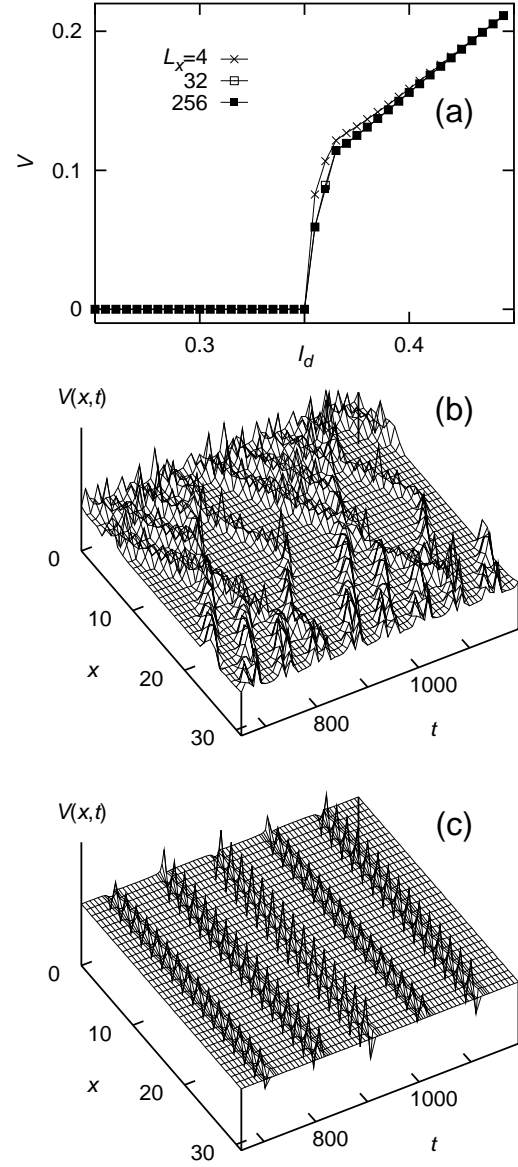


FIG. 3. (a) Time averaged voltage V per junction versus external current I_d for uniform-current (UC) injection case. The absence of finite-size effects for large sizes shows that $I_c = 0.350(1)$ is the true critical current. (b) Voltage $V(x,t)$ at time t across the horizontal junction at position x along a row of junctions for UC at $I_d = 0.36$: voltage pulses travel from the contacts into the sample. (c) $V(x,t)$ for the translationally invariant case at $I_d = 0.417$: the voltage occurs instantaneously across the whole sample corresponding to the rigid motion.

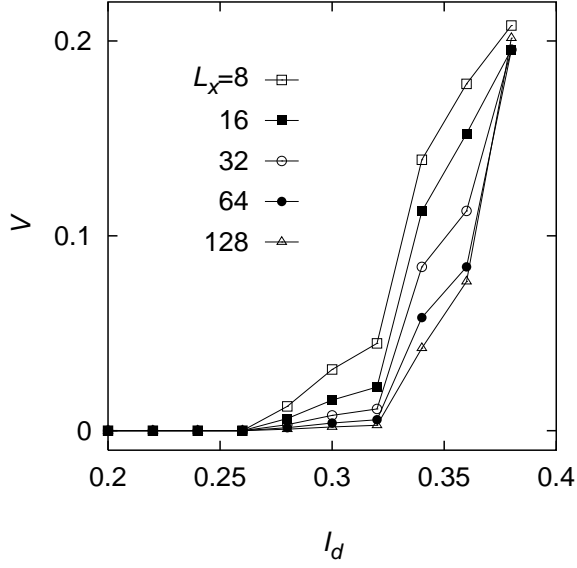


FIG. 4. Time averaged voltage V per junction versus external current I_d for the conventional busbar case [Fig. 1(b)]: V between the boundary critical current $I_{sb} \approx 0.28$ and the true critical current $I_c \approx 0.32$ vanishes as the distance between the contacts increases because it is due to the motion of the vortex columns closest to the contact. The onset of nonzero voltage across the sample requires the domino mechanism which sets in at $I_c \approx 0.32$.

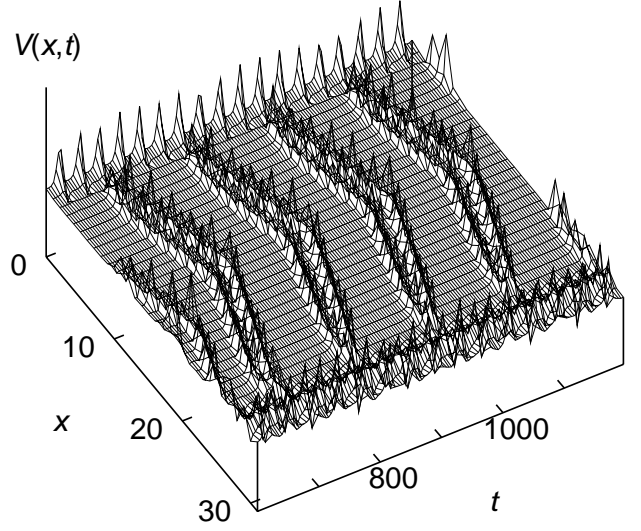


FIG. 5. Voltage $V(x, t)$ at time t across the horizontal junction at position x along a row of junctions for the IB2 case with inhomogeneities close to the contacts in Fig. 1(e) at $I_d = 0.416$. The critical current is in this case close to the upper limit given by the translationally invariant case, but the domino mechanism is still responsible for the onset of nonzero voltage.